Kinematic separation of mixtures

M. Goldshtik, H. S. Husain, and F. Hussain
Department of Mechanical Engineering, University of Houston, Houston, Texas 77204-4792
(Received 16 May 1991)

A phenomenon of spontaneous separation of components in an initially uniform fluid mixture is found experimentally. A qualitative explanation of the effect is proposed in terms of nonparallel streamlines in the medium.

PACS number(s): 47.15.Pn, 47.30.+s, 47.55.Kf

I. INTRODUCTION

To visualize flow patterns passive scalars, such as smoke in air or dye in liquid flows, are typically used. Such scalar particles follow fluid trajectories for a sufficiently long period of time. An impressive illustration of this feature is the well-known Taylor experiment [1]. A drop of dye in a glycerin solution between two cylinders appeared to be fully mixed when the inner cylinder was subjected to a few slow revolutions. However, the same number of inverse revolutions of the inner cylinder transformed the dye back to its initial state showing virtually no effects of diffusion. A modification of this process, including anomalous diffusion induced by chaotic Lagrangian dynamics, has been suggested for fine-scale separation of mixtures, for instance, of isotopes [2]. Lagrangian dynamics and chaos have become a major focus of fluid dynamics research in recent years [3,4].

However, we are unaware of any conjecture made so far that a uniform mixture of two species (say, smoke and air) can be separated by purely kinematic action. We have examined about 1500 published papers concerning diffusion and mixture separation, but have not found anything like the paradoxical separation of species we have observed in our experiments. Our experience in vortex flows and the mechanics of dispersed mixtures along with their visualizaton have led us to conjecture that kinematic separation of an initially uniform mixture is possible. This was the motivation of our experiment.

II. EXPERIMENTAL APPARATUS AND PROCEDURE

The experimental apparatus, shown in Fig. 1, consists of 91.5 cm-long glass cylinder of inner radius $R=7.62$ cm, and two bounding top and bottom plates. The top plate, whose height is adjustable, is fixed to the cylinder for this experiment. The bottom plate and the cylinder can be rotated independently in either direction. During the experiments, the domain was hermetically sealed so that fluid could neither enter nor leave the flow domain. In the present experiment, the height of the top plate was fixed at $H=13.97$ cm so that the aspect ratio H/R of the chamber was 1.83. The experiments were performed at a Reynolds number Re ($\equiv\Omega R^2/\nu$)$=2500$ (where Ω is the angular speed of the bottom plate, and ν the kinematic viscosity). Our study is based on flow visualization in air (uniformly laden with tobacco smoke) as well as in a glycerin-water solution (laden with low concentration of the fluorescent dye B1G1). The flow field was visualized by light from a 12-W Ar–ion laser. The laser beam was spread into a thin sheet about 0.5-mm thick using a cylindrical lens to illuminate the meridional plane of the flow field. A similar apparatus has been used by Escudier [5] to study the vortex breakdown phenomenon.

III. RESULTS

A. Vortex breakdown

Numerical simulations of the vortex breakdown phenomenon in such a system have been carried out by Lopez [6]. Experiments as well as calculations show a complex meridional circulation. Within a range of the Reynolds number Re and aspect ratio H/R, a sharp divergence of streamlines takes place near the symmetry axis, resulting in the development of an inner recirculating region popularly known as the vortex breakdown region or separation bubble. This is schematically shown in

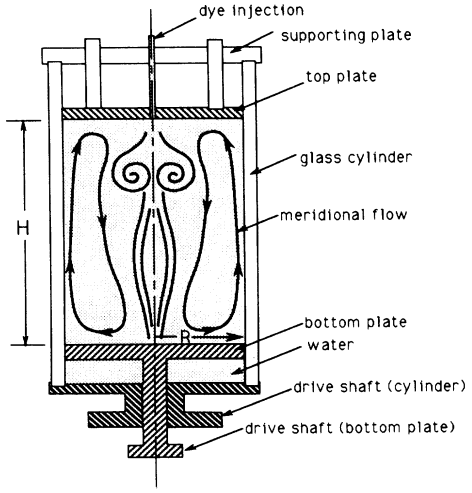

FIG. 1. Schematic of the flow facility.

Fig. 1. In the present experiment, the chosen parameters $H/R = 1.83$ and $\mathrm{Re} = 2500$ correspond to that which produces a single steady axisymmetric vortex breakdown. For stability boundaries of various flow patterns (including the number of vortex breakdowns) in the (Re, H/R) plane for a similar apparatus, see Fig. 7 of [5]. There are a variety of other forms of vortex breakdown, viz. spiral, nonaxisymmetric, unsteady, etc. [7], but in this paper we consider only axisymmetric vortex breakdown. This is the only type relevant to our study.

Figure 2 shows a typical flow visualization picture of the vortex breakdown obtained in our flow facility. In this case, fluorescent dye was introduced through a hole at the center of the top plate using a hypodermic needle, so that the dye seeped into the symmetry axis very slowly without producing any disturbances. This single axisymmetric vortex breakdown picture is similar to that observed by Escudier [5]. In this picture, the bright regions indicate the presence of fluorescent dye, while the dark regions correspond to glycerin-water mixture not reached by the dye. The contrast of light emitted by the fluid medium may serve as a measure of mixture concentration. A similar picture was also observed when we introduced smoke along the symmetry axis in air.

The flow in the chamber is a complex helical flow consisting of azimuthal and meridional flows. The rotating bottom plate acts as a centrifugal pump, imparting radial and azimuthal components of velocities to the fluid close to it. The cylinder wall guides upward flow advection, while the top plate turns the flow radially inward so that the flow first collapses into a slender vortex column before it descends and undergoes axisymmetric vortex breakdown. To gain a better perception about the flow in a meridional plane, the streamlines computed by Lopez [6] are reproduced in Fig. 3. The close agreement between the experiment and the simulation is impressive. Note that although the Reynolds numbers in the present experiment and the simulations of Lopez are almost the same (~ 2500), the aspect ratios are different, at this Re and the aspect ratio $H/R = 2.5$ used by Lopez two vortex breakdowns occur.

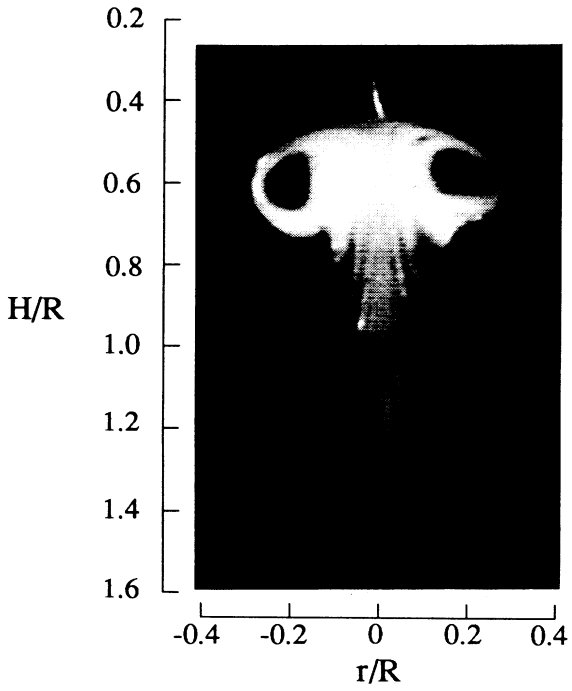

FIG. 2. A typical picture of vortex breakdown.

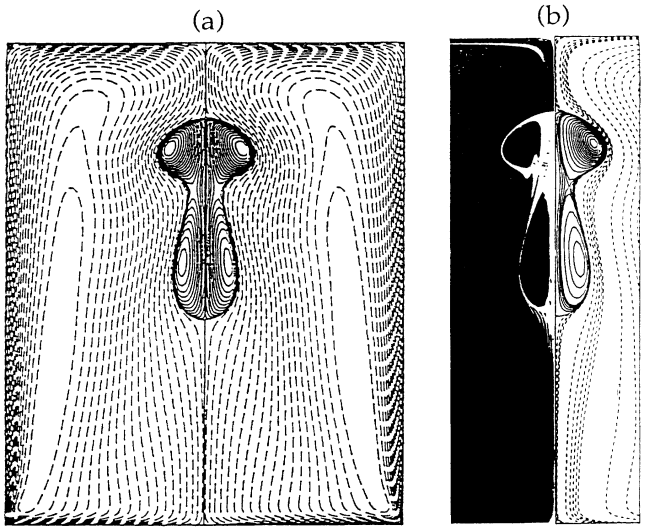

FIG. 3. Results of Lopez [6]. Computed streamlines in the meridional plane. (b) Comparison of visualization of the steady dye lines (left) and computed streamlines (right). $\mathrm{Re} = 2494$; $H/R = 2.5$.

B. Separation of mixture

During our experiments, we observed an unusual phenomenon. When a *well-mixed homogeneous mixture* of a passive marker and fluid is set into motion by rotating the bottom plate, a *nonuniform distribution* of flow markers develops. In this case, a visualization picture appears which is essentially the inverse of the picture shown in Fig. 2, i.e., the bright and dark regions interchange. The dark region near the axis of symmetry signifies the absence of flow markers, while the bright outer regions indicate an accumulation of flow markers.

We have observed the separation of markers in both cases of dye-glycerin-water and smoke-air mixtures. The initial uniform distribution of each mixture is obtained in our experiments either by holding the setup at rest for an extensive time or by convective mixing in which the bottom plate and the cylinder are rotated in opposite directions. In the latter case, the homogenization of the mixture occurs significantly faster.

The separation of dye markers in the glycerin-dye mixture seems to be much weaker than that observed in the smoke-air mixture. The glycerin-dye mixture solution

produced very low contrast between the dyed and undyed regions of the flow field. Thus no clear picture could be obtained. That is why we recorded the evolution of the separation process for the smoke-air mixture only.

A sequence of pictures selected form the recorded videotape is shown in Fig. 4. This sequence demonstrates a typical scenario in the development of nonuniform flow marker distribution. After only a few seconds, the initially uniform concentration of the mixture becomes nonuniform. Figure 4(a) exhibits the generation of a dark region near the upper part of the symmetry axis, signifying a depletion of smoke concentration in this region. The stages of development of the vortex breakdown region are characterized by the depletion of flow markers as shown in Figs. 4(b)–4(d). Figure 4(d) represents the steady-state picture of the flow field. A close-up view of the steady state's internal details is shown in Fig. 4(e). This steady state of the smoke-air mixture persists for an indefinite amount of time.

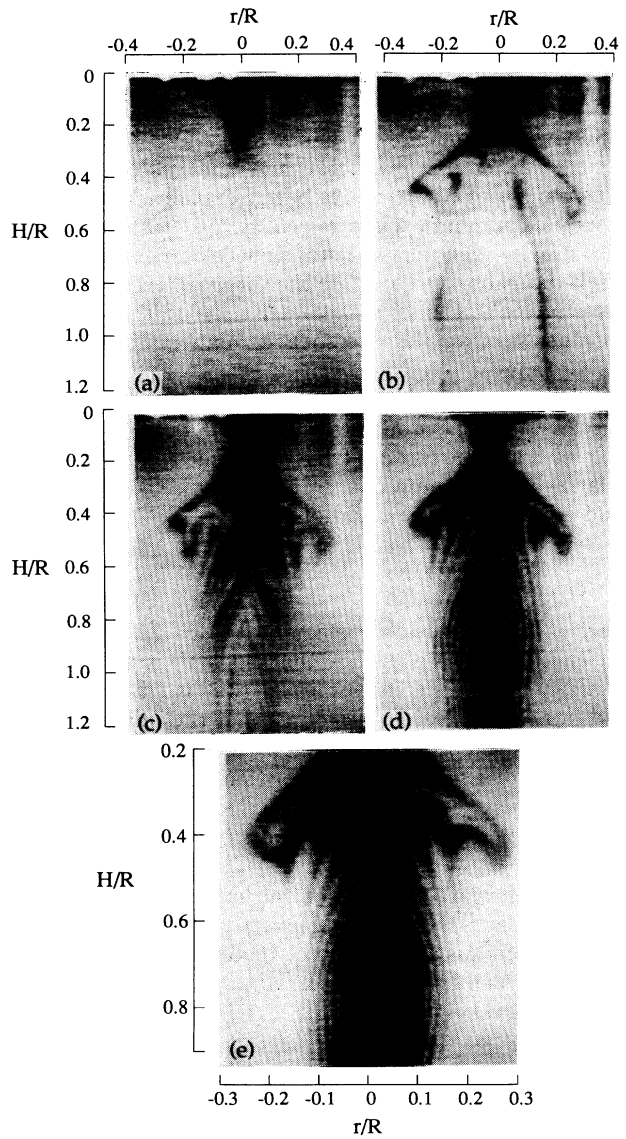

FIG. 4. Flow visualization pictures showing the smoke separation sequence. (a) $t=5$ s; (b) $t=20$ s; (c) $t=55$ s; (d) $t=70$ s; (e) $t=200$ s.

In addition to the dark area in the near-axis region, a thin marker-depleted layer is seen along the cylinder wall and top plate. This depleted layer is not clearly visible in the pictures shown in Fig. 4. It is apparent that while clear (i.e., smoke-depleted) air is transported by the meridional flow into the top near-axis region, the thickness of the depleted layer increases slowly along the wall. This suggests that continual separation of smoke occurs.

Note that although the overall images of the bubbles (recirculating regions) shown in Figs. 2 and 4 are similar, the internal details are quite different. The striations of marked and unmarked regions, especially in the wake region of the bubble (i.e., downstream of the vortex breakdown bubble), are more clearly visible in the case of initially uniform mixture of air and smoke than in the glycerin-water mixture (in which dye was introduced along the axis from the top plate). This difference in the visualized pictures are further discussed in Sec. IV.

The separation of smoke particles from air is found to be more dramatic when the cylinder and the top plate are rotated together in the same direction at half the bottom plate speed. In this case, a vortex column free of smoke particles is formed. A sequence of pictures illustrating the formation of the smoke-depleted column is shown in Fig. 5. Similar to the preceding case, the darker segments appear initially near the top plate and then propagate downward along the symmetry axis as a column. These segments are displaced from the axis, presumably because of the centrifugal pumping of the top plate. The lower part of the column shows a thin dark layer which protrudes out like "shoulders" [Figs. 5(b) and 5(c)]. As the vortex column extends downward, the shoulders show oscillations in the vertical direction. Finally, the column reaches the bottom, establishing the steady-state configuration of the smoke-free air column on the axis [Fig. 5(d)].

It must be stressed that a very important feature of all cases studied by us is that the characteristic time for the generation of the nonuniform distribution of markers from the uniform initial state is of the order of tens of seconds. This time scale seems to be identical to that for establishment of the steady hydrodynamical regime [6].

Evidently, the final mixture distribution in the steady state does not depend critically on the initial conditions. However, the distribution is strongly dependent on the variations of kinematic and dynamic parameters, viz., the ratio of angular velocities (of the bottom plate and the rest of the container) and the Reynolds number. In particular, if the angular velocities are the same, a rigid body rotation is established in the flow without any separation, and any initial nonuniformities of the marker distribution disappear with time. This observation belies the possibility that the centrifugal force field and barodiffusion phenomenon may be the cause of this separation process. Because of the small value of centrifugal acceleration (<0.5 g), the effect of centrifugal sedimentation (i.e., separation) is negligible.

The volume fraction of the marker has a profound effect on visualization of the separation process. When the initial marker concentration is very small, the separating region and the rest of the flow show little contrast. When the marker concentration was high, the contrast between the separated and unseparated regions was also poor (although the brightness of the observed plane increased). It appears that there is an optimum marker concentration which causes the most effective separation of the markers from the fluid, thus producing the highest contrast in the observed plane. Note that the characterization of concentration as "high" or "low," as we discuss here, is purely for discussion of visualization pictures. That is, even at this "high" concentration, it is still low enough to consider the smoke as a passive scalar; "high" concentration does not influence air motion as the streamline pattern remains unchanged from that for "low" concentration. But changes do take place with small variations of other parameters, such as the Reynolds number and the aspect ratio.

To eliminate the possibility of a buildup of electrostatic charges on the rotating surfaces which could cause separation through deposition of markers on the wall, we treated the solid surfaces with an antistatic solution. This did not change the separation process, confirming that the phenomenon is not a consequence of an electrostatic process; rather, it is a hydrodynamic effect.

For a fresh glycerin-dye mixture, we observed a separation process similar to that in the air-smoke case. The fluorescent dye used in our experiments had practically the same density as that of the background fluid. The volume concentration of the dye is negligibly small and has no influence on the solution characteristics. During the kinematic time period (i.e., time for flow establishment or spin-up time, typically around 1 min), the evolution of dye separation is similar to the pictures shown in Figs. 4 and 5. However, after a long time (of the order of a few hours) the sharpness of the picture became weaker and the dye distribution became uniform, as discussed below.

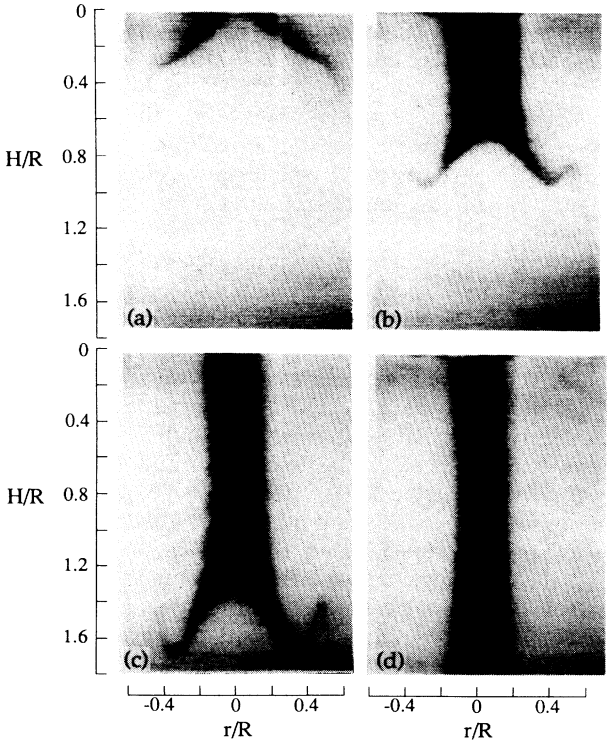

FIG. 5. Flow visualization sequence showing the development of the smoke-depleted column. (a) $t=20$ s; (b) $t=40$ s; (c) $t=60$ s; (d) $t=75$ s.

IV. TENTATIVE EXPLANATION

Analyzing the observed phenomenon, one may conclude that the most probable explanation for the separation is of a pure kinematic nature. This means that for a fairly short time scale, the influence of any force field, as well as diffusion and Brownian motion, may be neglected. In other words, the mixture particles of sizes such as 0.1 μm seem to be "frozen" in a fluid continuum, and their velocity coincides with the local fluid velocity. To understand the phenomenon, it is necessary to distinguish the motions of smoke particles and air molecules. The motion of smoke particles is better explained in terms of air as a continuum, while in reality air consists of molecules moving chaotically with high velocities and subject to self-diffusion. Because of the large difference in mass between smoke particles and air molecules, the coefficient of diffusion of smoke due to Brownian motion is much smaller than that of air.

However, the kinematic approach faces difficulties if one considers particle distributions in the framework of the classical theory of diffusion, which treats a passive scalar as a continuum characterized by its concentration c and governed by the equation

$$\frac{\partial c}{\partial t}+\mathbf{v}\cdot\nabla cd=\mathcal{D}\Delta c\ , \tag{1}$$

where $\mathcal{D}$ is the diffusion coefficient.

It is reasonable to assume that the wall is not the sink of mixture particles in our case; that is, the boundary condition at the wall is $\partial c/\partial n=0$. If the initial concentration c_0 is uniform, then Eq. (1) has a unique solution $c=c_0$ for all time. This means that in this theoretical sense, the separation phenomenon cannot be predicted. The same is also true in the limit $\mathcal{D}\to 0$, i.e., when the Brownian motion is neglected.

As an alternative, consider the mixture as a discrete system of particles following exactly the motion of the medium, which is assumed to be incompressible. The Lagrangian dynamics of a marked particle is governed by the dynamical system,

$$\frac{d\mathbf{x}}{dt}=\mathbf{v}(\mathbf{x},t),\quad \mathbf{x}(0)=\mathbf{x}_0\ , \tag{2}$$

where $\mathbf{v}(\mathbf{x},t)$ is the velocity field and the vector $\mathbf{x}_0$ corresponds to an initial position of the chosen particle. Contrary to Eq. (1), Eq. (2) is nonlinear and the trajectories can have complex behavior. In particular, the motion de-

scribed by (2) may be chaotic. For instance, this feature has been suggested in [2] to explain the separation process of a mixture, but in a qualitatively different process. In the limit $t \to \infty$, if the velocity field $\mathbf{v}(\mathbf{x},t)$ reaches a steady state, then the trajectories coincide with the streamlines.

In a typical case, diverging trajectories of system (2) may transform an initial uniform distribution of a discrete number of particles into a strongly nonuniform distribution. There exists a major difference between the discrete and continuum cases; in the continuum case, the divergence of trajectories does not lead to nonuniform density distribution. This can be explained by considering an incompressible flow from a point source in a plane. Imagine a uniform distribution of particles near the source which are placed at the grid points generated by a set of rays emanating from the source and circles centered at the source. Particle density along a ray increases with distance from the source, while its density decreases in the azimuthal direction. However, the fluid density remains constant everywhere in the flow field. Physically, this relates to the conservation of medium continuity by strong mobility of the fluid molecules participating in the isotropic chaotic motion. This explanation why the fluid molecules redistribute while the marked particles remain along the ray and become progressively denser. This difference in dynamics disappears if the mobility of the marked particles is comparable to that of the fluid particles. Possibly, this occurs in the glycerin solution where drops of dye become smaller by breakup and then dissolve, thus forming a homogeneous solution of dye and glycerin.

Such divergence of fluid trajectories takes place in our experiment. Assume that the particles are initially distributed uniformly in the fluid which is at rest. As the bottom plate begins to rotate, it drives a fluid motion which then becomes steady. In this situation, trajectories are transformed into streamlines. However, marked streamlines are placed in the space nonuniformly; they become more densely packed in regions of higher velocity and become more rare in regions of smaller velocity. In other words, the streamlines converge and diverge in different regions of the flow, and this leads to a nonuniform concentration of particles.

From the point of view of discrete particle concentration, an increase in the number of particles above a critical value decreases the image contrast. As the number of particles increases, an increasing number of streamlines are marked. In the limit, the marked streamlines cover the entire field, producing uniformly distributed markers in the flow field. This tentative explanation indicates that there exists an optimal concentration which results in the most effective separation of markers. A similar situation is encountered in photography. The sharpness of a picture on a photographic film depends nonmonotonically on the exposure time. That is, the contrast of a picture depends on the optimum exposure time, it is low both in exposed and underexposed pictures.

The above qualitative explanation deals mostly with the rapid establishment of the separation, but does not explain why the established regime does not depend on the initial distribution of particles. In seems reasonable that a different initial distribution should visualize a different set of streamlines and therefore should result in a different final distribution of particles. In the case of an air-smoke mixture, it is also not obvious why smoothing of the steady picture due to Brownian motion does not occur.

A probable reason for the smoothing of flow markers in the glycerin solution is discussed above. In the air-smoke mixtures, particle sizes do not change and this seems to cause different behavior.

The difference between the visualized pictures shown in Figs. 2 and 4 is believed to be due to the difference in the initial condition. In the smoke-air case, a large volume of smoke-depleted air produced in the boundary layer moves past the separating bubble. A part of the smoke-free air traveling from the top along the symmetry axis gets entrained in the bubble, while the rest of the off-axis free air moves over the bubble and advects downstream after passing through a larger cross section. Moreover, the diverging streamlines downstream of the bubble furthers the separation of smoke markers, producing sharp striations of dark and white layers. However, a detailed understanding of the separation mechanism requires further study.

In the glycerin-water mixture, the injected thin line of dye along the axis of symmetry is mostly entrained in the bubble; a small amount of off-axis dye marks a narrow region in the wake. Note that if we had introduced the dye at a different radial location and at a different depth, we would obtain a different picture. In such a case, the streamlines farther away from the axis of symmetry would be more visible. When the experiment with the introduced dye in the glycerin-water mixture was allowed to run for a moderate time, the transitional picture formed initially (i.e., showing a vortex breakdown pattern as in Fig. 2) became gradually more diffuse, and a steady-state picture was attained is very similar to that shown in Fig. 4. As already mentioned, if the apparatus is kept running indefinitely, the mixture of dye-glycerin-water becomes uniform because of dissolution.

It follows from the above discussion that the mechanism of separation cannot be explained only by an unsteady process. Some mechanism is needed to permanently sustain the separation of particles in steady conditions. This mechanism seems to be provided by the interaction of the flow and wall. Let us consider a steady boundary on a flat plate. This case is similar to the near-wall flow in Fig. 4(a) beginning at the lower corner between the bottom and the lateral wall where the streamlines move away from the wall with increasing upward distance due to viscous effects. If there is a uniform distribution of discrete particles upstream of the plate, then the concentration in the near-wall region decreases downstream. If we consider a particle nearest to the wall, the distance between this particle and the wall increases as it moves downstream. As a result, the space between the wall and the corresponding streamline appears as a region of "dark" fluid. We think the reasons are the same as explained for a source flow. Note that the initial uniform set of particles in the near-wall zone is quickly re-

moved during the unsteady processes of the boundary layer formation, in which the fluid velocities near the wall are large. After that, near-wall zone forever remains particle poor.

Note that the rotational motion of the flow in our chamber increases the effective length of the boundary layer substantially because of the spiral form of the streamlines. This is in agreement with the observed process in our experiments in which the "dark" regions initially are generated near the wall, accumulate near the top part of the symmetry axis, and then form the separating bubble on the axis. We think that the cause of the separation is due to the differences in the mobility of the marker particles and the fluid molecules. Particles of smoke are also subjected to diffusion due to Brownian interaction with molecules. However, a coefficient of particle diffusion is much smaller than the coefficient of self-diffusion of air as a result of the large ratio of particle mass to molecular mass of the fluid.

If our conjecture that the difference in the behavior of particles and fluid is caused by the different values of the diffusion coefficient is correct, then this effect can be used for separation of gas mixtures with different coefficients of individual components. However, this requires further detailed studies.

V. CONCLUDING REMARKS

The above explanation is both qualitative and intuitive and is not intended to be complete. Our results pointed out some limitations of the classical diffusion theory based on Eq. (1) in describing the behavior of the discrete system of particles observed in our experiments. In this case the Lagrangian approach based on Eq. (2) seems to be more relevant. Perhaps the explanation of the observed phenomenon can be obtained by some modification of the traditional continuum diffusion equation for binary mixtures with different mobility of its components. It seems that an appropriate test for the validity of a future theory would be its ability to describe the fine structure shown in Fig. 4.

In addition, we would like to make a conjecture that the observed phenomenon of kinematic separation of mixtures belongs to the same class of rather enigmatic phenomenon of the countergradient transfer that includes the well-known Ranque effect [8] which was discovered in 1932, but until now has remained poorly understood.

A question naturally arises as to the effect of the marker depletion reported here on the effectiveness of flow visualization with markers. We have repeatedly emphasized the limitation of flow visualization (even at the Schmidt number $Sc=1$) for three-dimensional flows such as turbulence and vortex interactions where dynamically dominant motions can be obscured by visualization [9,10]. In our present study, however, this visualization problem is nonexistent as we have here a distinctly different mechanism of marker depletion.

ACKNOWLEDGMENTS

The authors are thankful to Professor V. Shtern and Professor I. Kunin for illuminating discussions, and acknowledge the financial support of the Office of Naval Research under Grant No. N00014-89-J-1361 and the Department of Energy under Grant No. DE-FG05-88ER13839.

[1] G. I. Taylor, *Illustrated Experiments in Fluid Mechanics* (MIT, Cambridge, MA 1972), pp. 47–54.
[2] H. Aref and S. W. Jones, Phys. Fluids **A1**, 470 (1989).
[3] J. M. Ottino, *The Kinematics of Mixing: Stretching, Chaos, and Transport* (Cambridge University Press, Cambridge, England, 1989).
[4] *Topological Fluid Mechanics,* edited by H. K. Moffatt and A. Tsinober (Cambridge University Press, Cambridge, England, 1990).
[5] M. P. Escudier, Exp. Fluids **2**, 189 (1984).
[6] J. M. Lopez, J. Fluid Mech. **224**, 533 (1990).
[7] S. Leibovich, Annu. Rev. Fluid Mech. **10**, 221 (1978).
[8] M. Sibulkin, J. Fluid Mech. **12**, 269 (1962).
[9] J. E. Bridges, H. S. Husain, and F. Hussain, in *Whither Turbulence? Turbulence in the Crossroads,* edited by J. L. Lumley (Springer-Verlag, Berlin, 1990), pp. 132–151.
[10] M. V. Melander and F. Hussain, in *Topological Fluid Mechanics,* edited by H. K. Moffatt and A. Tsinober (Cambridge University Press, Cambridge, England, 1990), pp. 485–499.

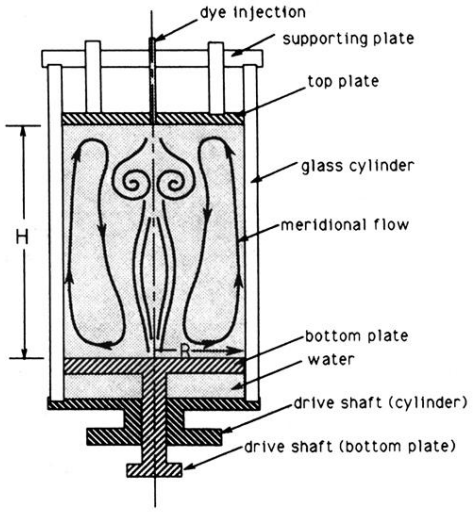

FIG. 1. Schematic of the flow facility.

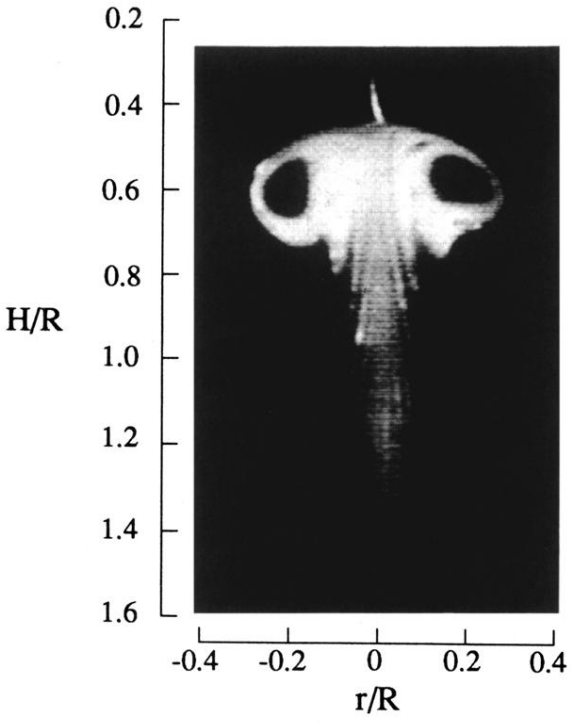

FIG. 2. A typical picture of vortex breakdown.

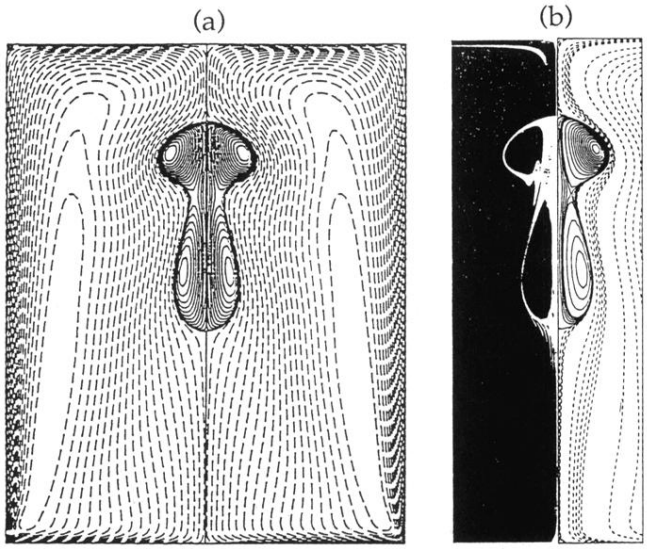

FIG. 3. Results of Lopez [6]. Computed streamlines in the meridional plane. (b) Comparison of visualization of the steady dye lines (left) and computed streamlines (right). Re=2494; $H/R=2.5$.

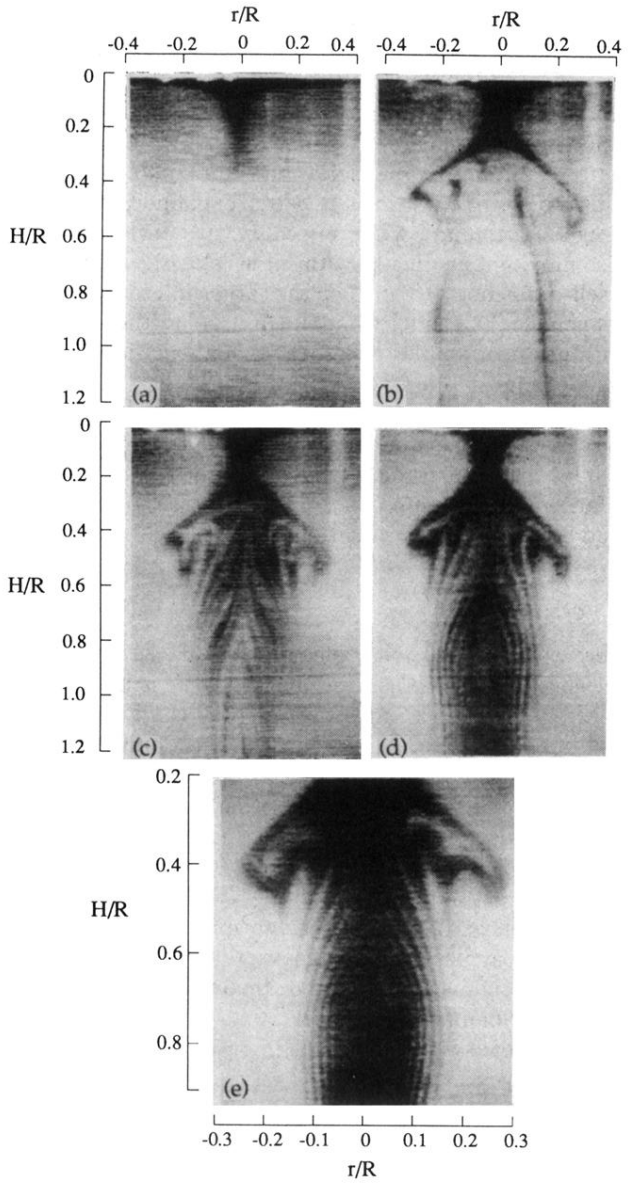

FIG. 4. Flow visualization pictures showing the smoke separation sequence. (a) $t = 5$ s; (b) $t = 20$ s; (c) $t = 55$ s; (d) $t = 70$ s; (e) $t = 200$ s.

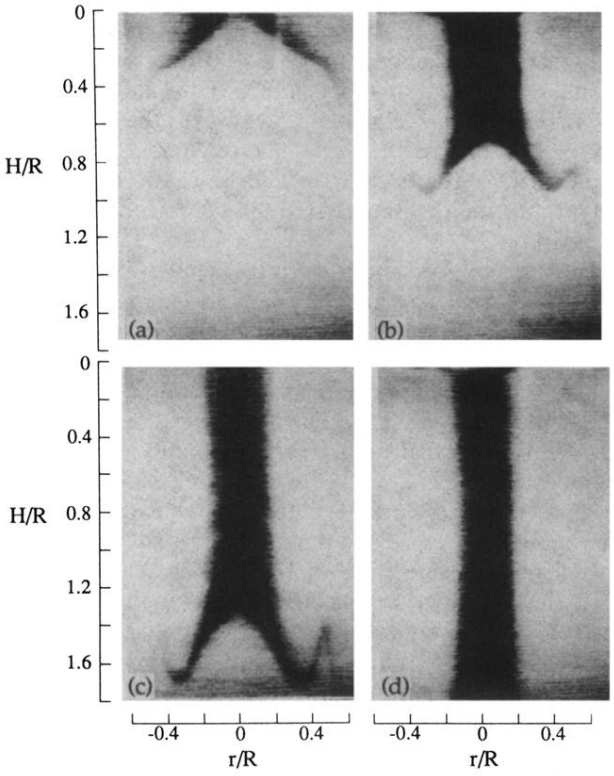

FIG. 5. Flow visualization sequence showing the development of the smoke-depleted column. (a) $t = 20$ s; (b) $t = 40$ s; (c) $t = 60$ s; (d) $t = 75$ s.